KnE Materials Science

MIE-2017
15th International School-Conference "New materials – Materials of innovative energy development, characterization methods and application''
Volume 2018

Knowledge E
Engaging minds

Conference Paper

Regularities of Changes in Structure and Texture of Low Modulus Alloy Zr-25Nb at Cold Rolling of Monocrystals with Different Orientations

M. Isaenkova[1], Yu. Perlovich[1], V. Fesenko[1], Ya. Babich[1], M. Zaripova[1], and N. Krapivka[2]

[1]National Research Nuclear University MEPhI (Moscow Engineering Physics Institute), Kashirskoe shosse 31, Moscow, 115409, Russia
[2]Institute of Problems of Strength by G.S. Pisarenko, Kiev, Ukraine

Abstract

The paper presents the results of studying the regularities of formation of the rolling texture in single crystals of Zr-25%Nb alloy, with different initial orientation relative to the external principal directions in the sheet: normal (ND) and rolling direction (RD). Varying the initial orientation of the single crystal made it possible to reveal stable orientations, among which are textural components {001} <100>, {001} <110>, {111} <110> and {111} <112>. For orientation <111> of single crystal, in the matrix of a quasi-single crystal it was possible to detect a finely dispersed ω-phase, which causes the appearance of an extended halo in the diffraction spectrum. The presence of ω-phase in the Zr-25%Nb alloy practically does not reduce the ductility of the material and does not affect the crystallographic texture formation mechanisms in bcc metals. Deformation of the β-alloy is carried out mainly by slip along the {112} <111> and {110} <111> systems. At deformation degrees of more than 80%, twinning along the {112} plane is observed, which is easily identified by the appearance of new textural maxima at characteristic distances from the initial ones.

Keywords: low-modulus Zr-25%Nb alloy, cold rolling, single crystal, crystallographic texture, deformation mechanisms

Corresponding Author:
M. Isaenkova
isamarg@mail.ru

Received: 21 December 2017
Accepted: 15 April 2018
Published: 6 May 2018

Publishing services provided by Knowledge E

Selection and Peer-review under the responsibility of the MIE-2017 Conference Committee.

1. Introduction

In work [1] it is shown that the use of implants made from low-modulus materials will improve the results of fractures treatment of long bones and reduce the percentage of postoperative complications. Taking into account the complexity of loads tested by the metal fixator installed in the femur, it is necessary to optimize the properties of the material in different directions. At present, alloys based on Ni-Ti alloys, characterized by excellent functional properties, are used as the material of implants. However,

recently it has been found that non-bound Ni atoms are ionized and propagated in a biological environment, as a result, the concentration of metal ions near the implant increases, which leads not only to a disruption in the supply of tissues directly in contact with the implant, that metal ions are distributed throughout the body [2]. Today, nickel and its alloys are banned in several countries for use in medicine, in particular, implants used in orthopedics and dentistry. Therefore, from the point of view of biochemical compatibility, Ni-Ti alloys should be replaced by more suitable alloys. The most promising is an alloy based on the Ti-Nb-Zr system, which is actively investigated in many countries of the world [3-7]. In this paper, the physical and mechanical properties of the Zr-25% Nb alloy, which is a promising alloy for metal fixers, are studied due to their high corrosion resistance, biocompatibility and low modulus of elasticity.

The purpose of this work is to reveal the mechanisms of plastic deformation and the ways of reorientation of single crystals of the low-modulus Zr-25% Nb alloy, which will allow understanding the possible limits of the variation of the crystallographic texture of the material to create the given properties.

2. Materials and methods

The Zr-25%Nb ingot was melted in a vacuum furnace in an argon atmosphere, then it was homogenized in a vacuum oven at 1000 °C for 3 hours. From the ingot using Bridgman method, single crystal was made. Parallel plates of different orientations were prepared by precise cutting of a single crystal, the list of which is given in Table 1. The dimensions of the samples were 4 mm x 4 mm x 3 mm. Further deformation of the samples was carried out by cold rolling to strain of 90% on a laboratory two-roll rolling mill. Taking into account the small dimensions of the sample and for the purpose of strictly observing the rolling direction (RD), the aluminum foil case was used.

The rolling was carried out with a deformation along the plate thickness of 5-10% per pass. At each successive stage of rolling, the dimensions of the initial sample were measured; the diffraction spectrum was recorded; the curves of instrumented indentation measured the mechanical characteristics (microhardness, modulus of elasticity with use of unloading curve and the share of plastic deformation in the area under the curve); the crystallographic orientation of the sample was evaluated by recording the direct pole figures {110}, {100} and {112} with which the orientation distribution function (ODF) was reconstructed using the LABOTEX software [8-9] and the coordinates of the normal direction (ND) and RD on stereographic projection. The

substructure state of the material from the half-width of the x-ray lines (FWHM - full width of half maximum) and the value of the unit cell parameter *a* was estimated.

Table 1: Rolled samples of a single crystal of the Zr-25Nb alloy.

Sample	Initial orientation	ε_{max}, %	Final orientation	Deformation system *
1	{368} < $\bar{1}2$ 2 3>	80 91	{111} < $\bar{2}$11>; {211} < $\bar{2}$13>; {111} < $\bar{2}$11>; {001} <110>;	{11$\bar{2}$} <111> twinning
2	{134} <1 11 15>	80 91	({111} < $\bar{1}$10> {111} < $\bar{1}$10> {111} < $\bar{2}$11>	Any slip system + twinning
3	{001} <001>	91	{001} <13 6 0>; {001} <14 3 0>	Any slip system + twinning
4	{001} <011>	90	{001} <011>	Any
5	{111} <11$\bar{2}$ >	95	{111} <11$\bar{2}$ > {100} <011>	Any slip system + twinning; {11$\bar{2}$} <111>
6	{111} <01$\bar{1}$ >	96	{111} <01$\bar{1}$ > weak {100} <011>	Any slip system + twinning
7	{011} <001>	95	{011} <001> {111} <11$\bar{2}$ > {332} <11$\bar{3}$ >	Any slip system {11$\bar{2}$} <111> {123} <11$\bar{1}$ >
8	{011} <01$\bar{1}$ >	95	{111} < $\bar{1}$10>; {111} <11$\bar{2}$ > {001} <100>	Any slip system + twinning
9	{011} <35$\bar{5}$ >	96	{011} <35$\bar{5}$ >; {111} < $\bar{3}$21>; {001} <110>	{123} <11$\bar{1}$ >+ twinning
10	{1$\bar{1}$0} <113>	90	{1$\bar{1}$1} <132> {1$\bar{1}$0} <117>	{11$\bar{2}$} <111> {123} <11$\bar{1}$ > {110} <1$\bar{1}$1>
11	{011} <2$\bar{1}$1>	91	{011} <3$\bar{1}$1>; {111} < $\bar{3}$12>	{123} <11$\bar{1}$ > {11$\bar{2}$} <111> {123} <11$\bar{1}$ >
12	{011} <11$\bar{1}$ >	90	{011} <21$\bar{1}$ >; {111} < $\bar{1}$10>	Any slip system
15	{112} <11$\bar{1}$ >	91	{111} <01$\bar{1}$ > {100} <01$\bar{1}$ >	{11$\bar{2}$} <111>
16	{112} < $\bar{1}$10>	90	{111} < $\bar{1}$10>	{11$\bar{2}$} <111>
17	{112} < $\bar{3}$11>	80	{111} < $\bar{3}$21>	{11$\bar{2}$} <111>
18	{112} <20$\bar{1}$ >	80	{111} < $\bar{2}$11> {100} <010>	{11$\bar{2}$} <111>

* – The most probable slip systems for the bcc structure are {011} <1$\bar{1}$1>, {11$\bar{2}$} <111> and {123} <11$\bar{1}$ > and twinning along {112}.

X-ray analysis was performed on the DRON-3 and D8 Discover diffractometers with Cr and Cu anodes, respectively. Primary data processing was carried out using software

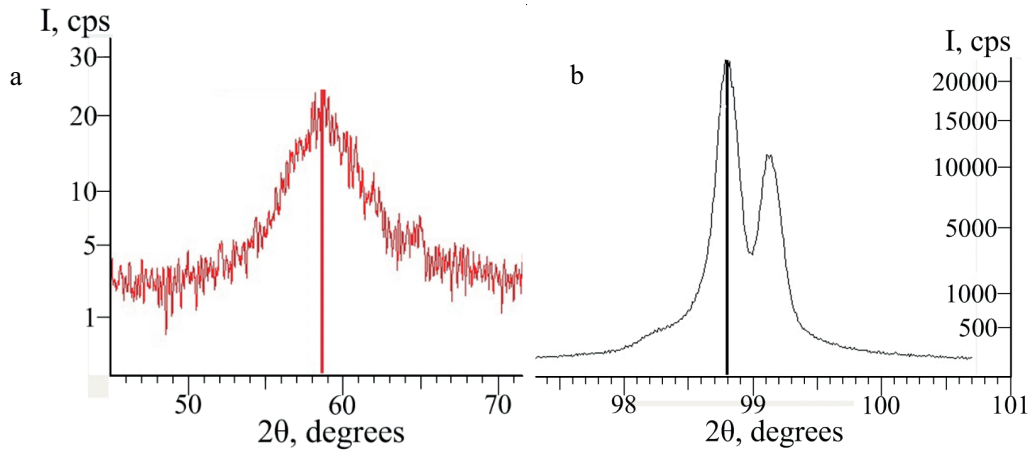

Figure 1: The lines of the diffraction spectrum for the ω-phase – (0002) (a) and for the β-phase – (222) (b), recorded for the {111} plane of a single crystal.

developed in the laboratory [10-11], as well as licensed software provided by Brooker to the diffractometer D8 Discover.

3. Results and discussion

The individual lines of the diffraction spectrum recorded for a single crystal with a {111} plane shown on Figure 1. The presence of a halo may indicate the presence of an amorphous phase in studied material. However, when single crystals of all other orientations are taken in the initial state, no such halo appears on the diffraction spectra and reappears when the {111} plane approaches the plane of the ND plate, although the amorphous phase in independent of direction. The angular position of halos, located near the Bragg angles 2θ, approximately to 59°, correspond to the angular positions of X-ray reflections (0002) from the basal plane of the ω-phase. In addition, according to [12], the orientation relation is realized between the β and ω-phases, due to parallelism of the planes $(0001)_{\omega}$ and $\{111\}_{\beta}$. Therefore, in the initial single crystal, there is dispersion segregation of the ω-phase, as can be seen from the observed wide halo, which extends 16 degrees along the Bragg scale. The halo width at the half height of the maximum intensity of the line is about 5 degrees. The presence of such a halo indicates the fineness of the ω-phase precipitates coherently and coupled to the matrix. The presence of the ω-phase was fixed only because of its strict orientation dependence with respect to the {111} β-phase planes.

The presence of a halo corresponding to the presence of a finely dispersed ω-phase was recorded on the diffraction spectra of a single crystal with the original orientation

{111} <11$\bar{2}$ > rolled up to the maximum deformation degrees (Fig. 2). We would like to note that the minimal plasticity is observed for this crystal.

In Fig. 3 shows the change in the direct pole figures {110} and {100} in successive stages of the plastic deformation of a single crystal with the initial orientation of the {368} < $\bar{1}$2 2 3>, as well as a change in the orientation of the ND and RD within the standard stereographic triangle. The continuous arrows show a reorientation of the chosen direction (RD or ND) as a result of slip, and the dashed arrows show a reorientation during twinning. The initial position of the ND and RD is shown in Fig. 3-d and 3-f with a black dot, and the intermediate positions are shown with hollow dots.

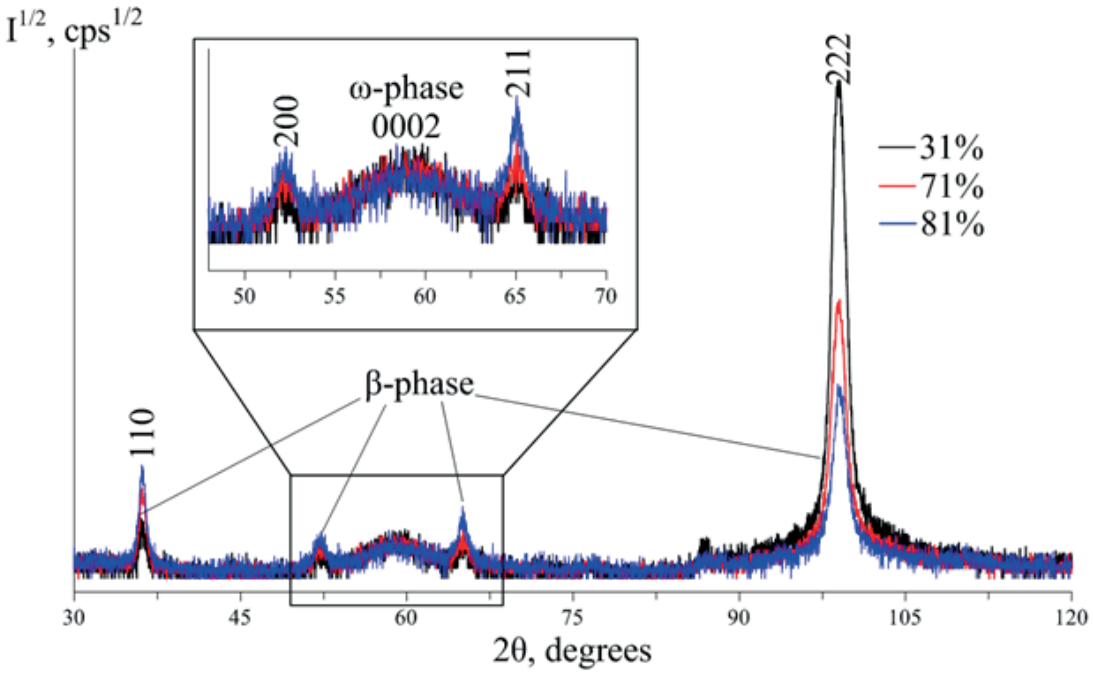

Figure 2: Diffraction spectra of a single crystal of Zr-25% Nb alloy with an {111} <11$\bar{2}$ > orientation, rolled to different degrees of deformation (31, 71 and 81%).

For all the samples studied in Table 1, as well as for the polycrystalline sample No. 13, results similar to those shown in Fig. 3. The main regularities of the reorientation of the ND and RD along the stereographic triangle, obtained on the basis of a detailed analysis of the behavior of single crystals of different orientations, are shown in Fig. 4, and specific final orientations of the rolled single crystal and possible mechanisms of deformation are listed in Table 1.

The presence in the Zr-25% alloy of the Nb ω-phase practically does not reduce the plasticity of the material and does not affect the crystallographic texture formation mechanisms inherent in bcc metals. Deformation of the β-alloy is carried out mainly by sliding through the systems {112} <111> and {110} <111>. At deformation degrees of more than 80%, twinning along the {112} plane is observed, which is easily identified

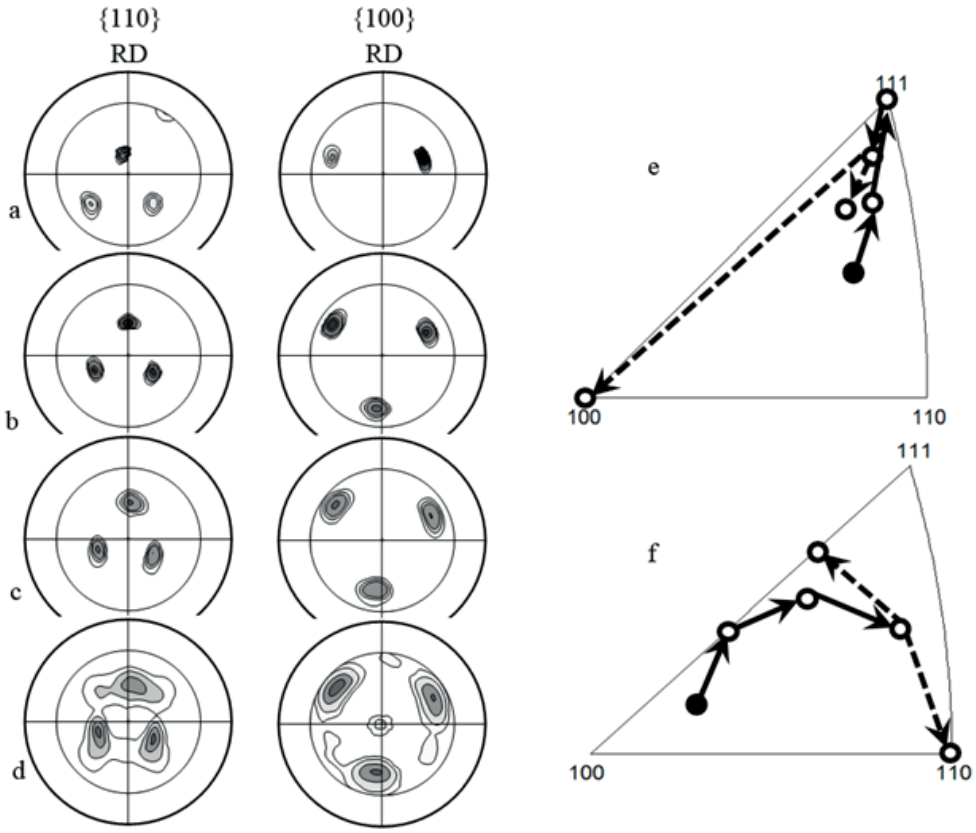

Figure 3: Development of the rolling texture in a single crystal with {368} < $\overline{12}$ 2 3> orientation (sample 1 in Table 1): a-d) pole figure {100} and {110} for the degrees of deformation ε = 21, 61, 80, 91%; e, f) reorientation of ND (e) and RD (f) within the standard stereographic triangle. Continuous arrows indicate a reorientation in the case of an {112} <11$\bar{1}$ > slip system, while dashed arrows indicate a twinning.

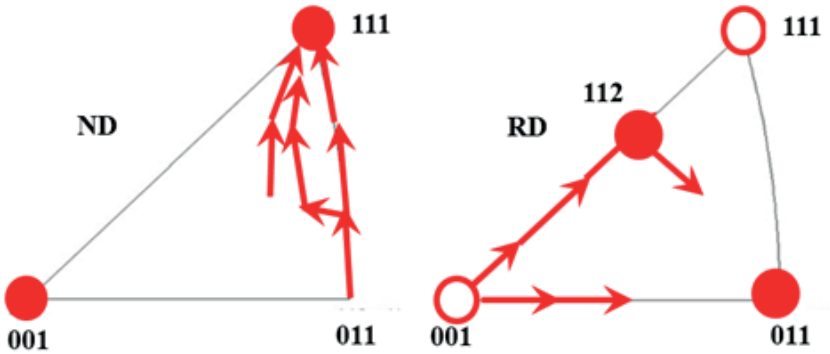

Figure 4: Regularities of the reorientation of ND and RD within the limits of standard stereographic triangles at the rolling of single crystals of different orientations: filled points characterize the stable textural components of ND and RD, and the hollow points are unstable.

by the appearance of new textural maxima at characteristic distances from the initial ones (Fig. 3-e, f).

According to the results of the analysis of the substructure state a monotonic grow of the line width (Fig. 5) is observed. This indicates an increase in the distortion of the crystalline structure of the material and its finely dispersed nature. In the case of

activation of twinning in the sample for deformations of more than 80%, an additional increase in the half-width of the line is observed (see Fig. 5), registered on all graphs to a greater or lesser degree. The maximum hardening of the material is observed for orientation {111}.

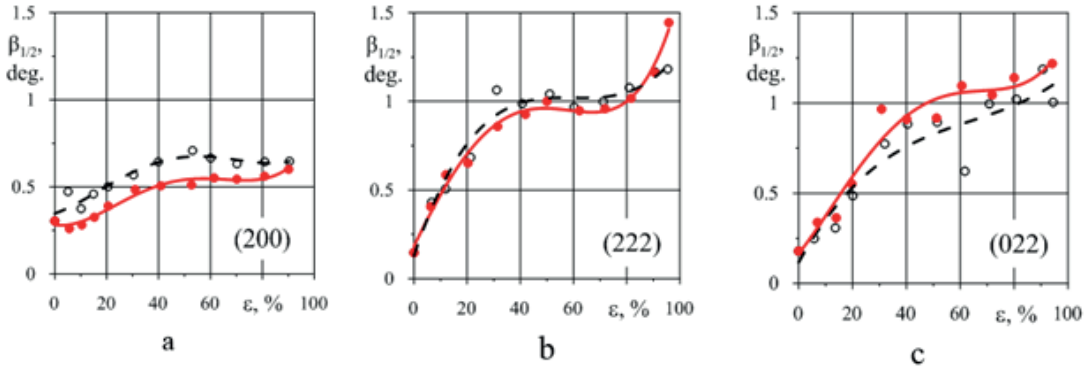

Figure 5: Change of half-widths (FWHM) of lines (200), (222) and (220) with increasing degree of deformation of single crystals of different initial orientations: a) –-{001} <001> and ——– {001} <011>; b) –– {111} <11$\bar{2}$ > and ——– {111} <01$\bar{1}$ >; c) –– {011} <001> and ——– {011} <01$\bar{1}$ >.

The distortion and crushing of the crystal structure leads to hardening of the material, and therefore the microhardness should increase at the same time with the increase in the half-width of the lines. However, the microhardness and half-widths of the x-ray lines (compare Fig. 5 and 6) show a monotonic increase in the microhardness for rolling only for certain orientations (Fig. 6-a), while for other initial orientations the microhardness changes according to sinusoidal law (Fig. 6-b, c). Probably, this behavior of the microhardness is connected to the mechanisms of plastic deformation acting during rolling.

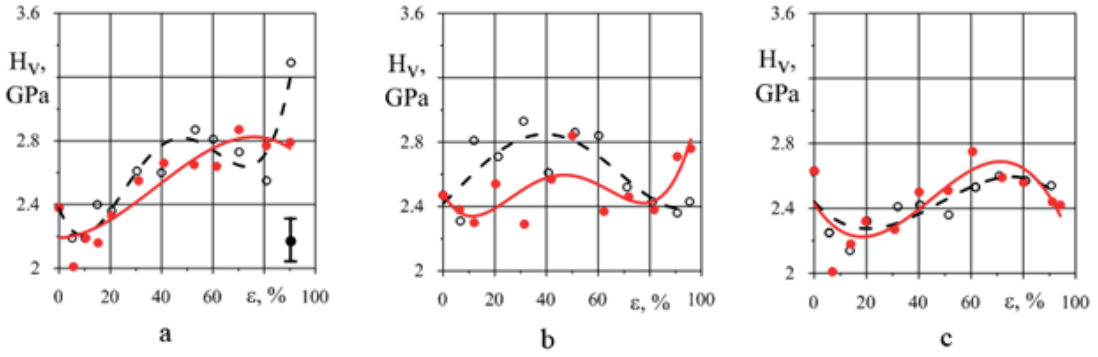

Figure 6: Change in microhardness with increasing degree of deformation of single crystals of different initial orientations: a) –-{001} <001> and ——– {001} <011>; b) –– {111} <11$\bar{2}$ > and ——– {111} <01$\bar{1}$ >; c) –– {011} <001> and ——– {011} <01$\bar{1}$ >.

4. Conclusions

1. It was found that the texture formation in the investigated mono- and polycrystalline Zr-25% Nb alloy develops in accordance with the typical laws for most BCC metals in which the main stable components of rolling texture are {001} <110> and $\{1\bar{1}1\}$ <110-112>.

2. When the Zr-25% Nb alloy is cold rolled, the textural component {001} <110> is stable at the strain less than 80%, and when the degree of deformation is increased to 90-98%, the components $\{1\bar{1}1\}$ <110-112> begin to predominate.

3. It is shown, that the initial single crystal of the Zr-25% Nb alloy, in fact, is not a single crystal, but it is a single-crystal matrix, in which numerous fine-dispersed inclusions of the ω-phase are distributed, creating extended halos in the diffraction spectrum of the sample.

4. The presence in the Zr-25% Nb alloy of the additional ω-phase practically does not affect the crystallographic mechanisms of texture formation, but promotes the plastification of the alloy, which indicates the location of dispersed particles in intergranular layers.

5. At the final stages of rolling, i.e. at a deformation of more than 80%, a twinning process is observed, as a result of which isolated textural maxima appear on the DPF and IPF, which were absent in the previous stage of rolling.

The work was carried out within under Governmental Support of Competitive Growth Program of NRNU MEPhI (agreement No.02.a03.21.0005) and Council on grants of the President of the Russian Federation.

References

[1] Yuhimchuk A, Kalashnikov A. Computer modeling of stress and deformation of the femur using intramedullary metal retainers of various elasticity. - Bulletin of orthopedics, traumatology and prosthetics, 2015, 3, p. 56-62.

[2] Gotman I. Characteristics of Metals Used in Implants 11 Journal of endourology. 1997. V. 11, № 6. P. 383-388.

[3] Miyazaki S, Kim HY, Hosoda H (2006) Development and characterization of Ni-free Ti-base shape memory and superelastic alloys. Mater Sci Eng A 438–440:18–24

[4] Bertrand E, Gloriant T, Gordin DM, Vasilescu E, Drob P, Vasilescu C, Drob SI (2010) Synthesis and characterization of a new superelastic Ti–25Ta–25Nb biomedical alloy. J Mech Behav Biomed Mater 3:559–564

[5] Brailovski V, Prokoshkin S, Gauthier M, Inaekyan K, Dubinskiy S, Petrzhik M, Filonov M (2011) Bulk and porous metastable beta Ti–Nb–Zr(Ta) alloys for biomedical applications. Mater Sci Eng C 31:643–657

[6] Yu. A. Perlovich, M Isaenkova, S Chekanov, V Fesenko, Krymskaya O. Superelastic alloy Ti-22%Nb-6%Zr: X-ray study of deformation features – IOP Conf. Series: Materials Science and Engineering 130 (2016) 012034 doi:10.1088/1757-899X/130/1/012034

[7] Zhang JY, Sun F, Hao YL, Gozdecki N, Lebrun E, Vermaut P, Portier R, Gloriant T, Laheurte P, Prima F (2013) Influence of equiatomic Zr/Nb substitution on superelastic behavior of Ti–Nb–Zr alloy. Mater Sci Eng A 563:78–85

[8] Pawlik K. Determination of the orientation distribution function from pole figures in arbitrarily defined cells, phys. stat. sol. (b) 134, 477 (1986)

[9] Jura J., Pospiech J. The Determination of orientation distribution function from incomplete pole figures, J.Textures of Crystalline Solids, 1978, vol.3, pp. 1-25.

[10] Isaenkova, M., Perlovich, Y., Fesenko, V. Modern methods of experimental construction of texture complete direct pole figures by using X-ray data IOP Conf. Series: Materials Science and Engineering 130 (2016) 012055 doi:10.1088/1757-899X/130/1/012055.

[11] Isaenkova M.G., Perlovich Yu.A., Krymskaya O.A., Fesenko V.A., Babich Y.A. Optimization of the procedure for determining integral texture parameters of products from zirconium-based alloys using the orientation distribution function - IOP Conf. Series: Materials Science and Engineering 130 (2016) 012056 doi:10.1088/1757-899X/130/1/012056

[12] Dobromyslov A, Taluc N. Structure of zirconium and its alloys. – Ekaterinburg, 1997. - 228 p.

[13] Perlovich Y., Isaenkova, M., Fesenko V., Krymskaya O. Texture Evidences of Interaction between Plastic Deformation and Phase Transformations in Zr-based Alloys. Materials Science Forum Vol. 702-703, 2012, pp.283-286.